In the format provided by the authors and unedited.

Localization of microscale devices in vivo using addressable transmitters operated as magnetic spins

Manuel Monge [1], **Audrey Lee-Gosselin**[2], **Mikhail G. Shapiro** [2]* and **Azita Emami**[1]*

[1]Division of Engineering and Applied Sciences, California Institute of Technology, Pasadena, CA 91125, USA. [2]Division of Chemistry and Chemical Engineering, California Institute of Technology, Pasadena, CA 91125, USA. *e-mail: mikhail@caltech.edu; azita@caltech.edu

In the format provided by the authors and unedited.

Localization of microscale devices in vivo using addressable transmitters operated as magnetic spins

Manuel Monge [1], Audrey Lee-Gosselin[2], Mikhail G. Shapiro [2]* and Azita Emami[1]*

[1]Division of Engineering and Applied Sciences, California Institute of Technology, Pasadena, CA, 91125, USA. [2]Division of Chemistry and Chemical Engineering, California Institute of Technology, Pasadena, CA, 91125, USA. *e-mail: mikhail@caltech.edu; azita@caltech.edu

In the format provided by the authors and unedited.

Localization of microscale devices in vivo using addressable transmitters operated as magnetic spins

Manuel **Monge** [1], Audrey **Lee-Gosselin**[2], Mikhail G. **Shapiro** [2]* and Azita **Emami**[1]*

[1]Division of Engineering and Applied Sciences, California Institute of Technology, Pasadena, CA, 91125, USA. [2]Division of Chemistry and Chemical Engineering, California Institute of Technology, Pasadena, CA, 91125, USA. *e-mail: mikhail@caltech.edu; azita@caltech.edu

SUPPLEMENTARY MATERIAL

Localization of Microscale Devices *In Vivo* using Addressable Transmitters Operated as Magnetic Spins

Manuel Monge[1], Audrey Lee-Gosselin[2], Mikhail G. Shapiro[2*], Azita Emami[1*]

[1]Division of Engineering and Applied Sciences,

[2]Division of Chemistry and Chemical Engineering

California Institute of Technology, Pasadena, CA, USA 91125

*Correspondence: azita@caltech.edu or mikhail@caltech.edu

I. Theoretical Spatial Resolution

II. Angular Misalignment

Supplementary Figure S1 – ATOMS localization

Supplementary Figure S2 – 3-D localization schemes

Supplementary Figure S3 – Compensation scheme for angular misalignment

I. THEORETICAL SPATIAL RESOLUTION

Consider an ATOMS device inside a body in a magnetic field profile $B_Z = g(x)$ as shown in **Figure S1**. The location of ATOMS can be estimated by mapping the magnetic field back in space according to

$$\hat{x} = g^{-1}\left(\frac{\Delta f + \Delta f_0}{\gamma_{ATOMS}}\right), \tag{S1}$$

where g^{-1} is the inverse function of B_Z, Δf is the frequency shift, Δf_0 is the frequency shift offset, and γ_{ATOMS} is the gyromagnetic ratio of the ATOMS device. To calculate the spatial resolution Δx for frequency encoding, we first take the derivative of Eq. (S1) and, using the inverse function theorem, we obtain

$$\hat{x}' = \frac{1}{g'(x)} = \frac{1}{G_Z}, \tag{S2}$$

where $G_Z = dB_Z/dx$ is the magnetic field gradient of B_Z. The spatial resolution is then given by

$$\Delta x = \frac{\Delta f_{\min}}{\gamma_{ATOMS}\, G_Z}, \tag{S3}$$

where we define $\Delta f_{\min} = 2\sigma_f$ as the minimum detectable frequency shift. σ_f is the standard deviation of the oscillation frequency and is defined as

$$\sigma_f = \sqrt{(\gamma_{ATOMS}\, \sigma_{MS})^2 + \sigma_{PN}^2}, \tag{S4}$$

where σ_{MS} is the magnetic sensor noise and σ_{PN} is the standard deviation of the oscillator's phase noise. Since the dominant noise source close to the oscillation frequency is flicker noise, the phase noise profile of the oscillator $S_\phi(\omega)$ can be approximated by a Gaussian profile in this region[1–3]. Thus, its standard deviation can be estimated by $\sigma_{PN} \approx FWHM_{S_\phi}/2.355$, where $FWHM_{S_\phi}$ is the full width at half maximum or 3-dB bandwidth of $S_\phi(\omega)$.

II. ANGULAR MISALIGNMENT

In the case of an angular misalignment of $\theta°$ degrees between B_Z and an ATOMS device (**Fig. S3a**), the measured magnetic field will be proportional to the projection of B_Z into the plane orthogonal to the device (i.e., $B_Z \cos\theta$), and can reduce the accuracy of the system. The polar angle ξ, in contrast, will not affect the resolution because the device only measures the orthogonal magnetic field. To overcome this limitation, we devise the following method which can be applied to frequency and phase encoding. We add an extra step in the pulse sequence where a uniform magnetic field B_C is applied to measure a

28 correction factor and correctly estimate B_{G_Z}, the local magnetic field at the device's location generated by

29 the field gradient G_Z.

30 **Figure S3b** shows the pulse sequence for localization of a single ATOMS device with angular

31 misalignment. We first apply the known field B_C. In this case, the ATOMS device measures $B_{MC} =$

32 $B_C \cos \theta$, which is estimated from the measured frequency shift by

$$B_{MC} = \frac{\Delta f_{MC}}{\gamma_{ATOMS}}, \tag{S5}$$

34 where Δf_{MC} is the frequency shift due to B_{MC}. Then, the angular misalignment can be estimated by

$$\theta = \cos^{-1}\left(\frac{B_{MC}}{B_C}\right). \tag{S6}$$

36 Second, we apply G_Z and the chip measures $B_{MZ} = B_{G_Z} \cos \theta$. Similarly, B_{MZ} is estimated by

$$B_{MZ} = \frac{\Delta f_{MZ}}{\gamma_{ATOMS}}, \tag{S7}$$

38 where Δf_{MZ} is the frequency shift due to B_{MZ}. Finally, combining the device's measurements B_{MC} and

39 B_{MZ} with equations (S5) and (S7) gives

$$\frac{B_{MZ}}{B_{MC}} = \frac{B_{G_Z} \cos \theta}{B_C \cos \theta} = \frac{\Delta f_{MZ}/\gamma_{ATOMS}}{\Delta f_{MC}/\gamma_{ATOMS}}, \tag{S8}$$

$$B_{G_Z} = B_C \frac{\Delta f_{MZ}}{\Delta f_{MC}}. \tag{S9}$$

42 This approach allows the correct estimation of the ATOMS device's location and also enables the

43 estimation of its orientation as long as the local magnetic fields B_{MC} and B_{MZ} are above the noise floor of

44 the magnetic sensor. This means

$$B_C \cos \theta \text{ or } B_{G_Z} \cos \theta > B_{\min}, \tag{S10}$$

46 where $B_{\min}$ is the resolution of the magnetic sensor. Therefore, the maximum angular misalignment $\theta_{\max}$

47 is given by

$$\theta_{\max} = \cos^{-1}\left(\frac{B_{\min}}{B_{G_Z\min}}\right), \text{ with } B_{G_Z\min} < B_C, \tag{S11}$$

49 where $B_{G_Z\min}$ is the minimum magnetic field generated by the field gradient G_Z.

50 For a single device, Δf_{MC} and Δf_{MZ} can be obtained in two successive acquisitions. For localization of

51 multiple arbitrarily arranged ATOMS devices (**Fig. S3c**), the device can calculate the alignment

52 correction internally (on-chip). In this scenario, both B_C and G_Z are applied consecutively so that the

53 devices measure B_{MC} and B_{MZ}. Then, each device calculates the ratio of B_{MC} and B_{MZ} and shifts its

54 oscillation frequency according to

$$\Delta f = \alpha \frac{B_{MZ}}{B_{MC}} \gamma_{ATOMS} = \alpha \frac{B_{GZ}}{B_C} \gamma_{ATOMS}, \tag{S12}$$

56 where α is a constant pre-programmed into the device which is set by the target bandwidth utilization.

57 Thus, the location of each device is estimated as described above.
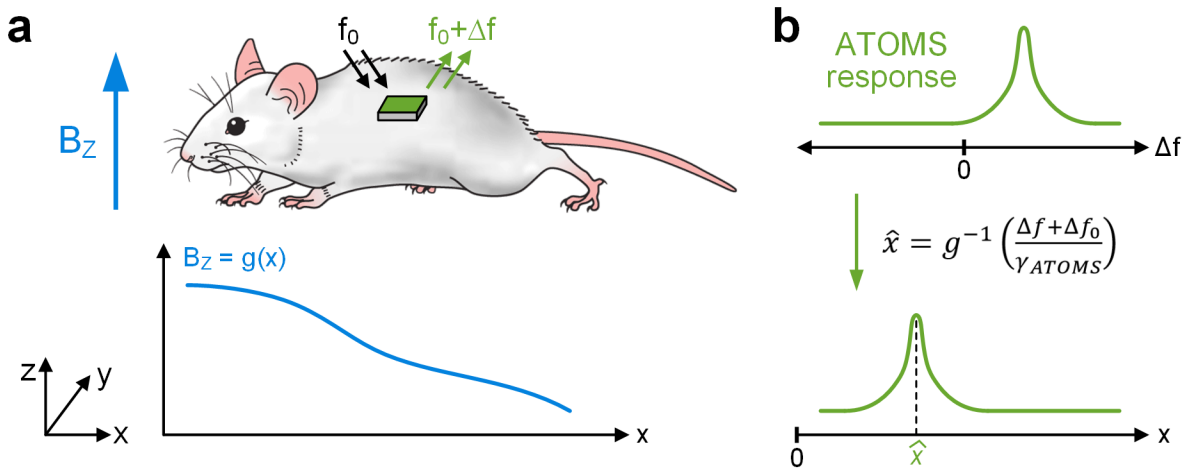
Supplementary Figure S1 – ATOMS localization. Illustration of the localization process of an ATOMS device inside the body of an animal or patient. (**a**) The ATOMS chip responds to the excitation RF signal by transmitting a signal with a frequency shift Δf proportional to the magnetic field generated by $B_Z = g(x)$ at the device's location. (**b**) The chip's response is used to estimate its location by mapping the magnetic field back in space according to Δf, its gyromagnetic ratio γ_{ATOMS} and the inverse function g^{-1}.
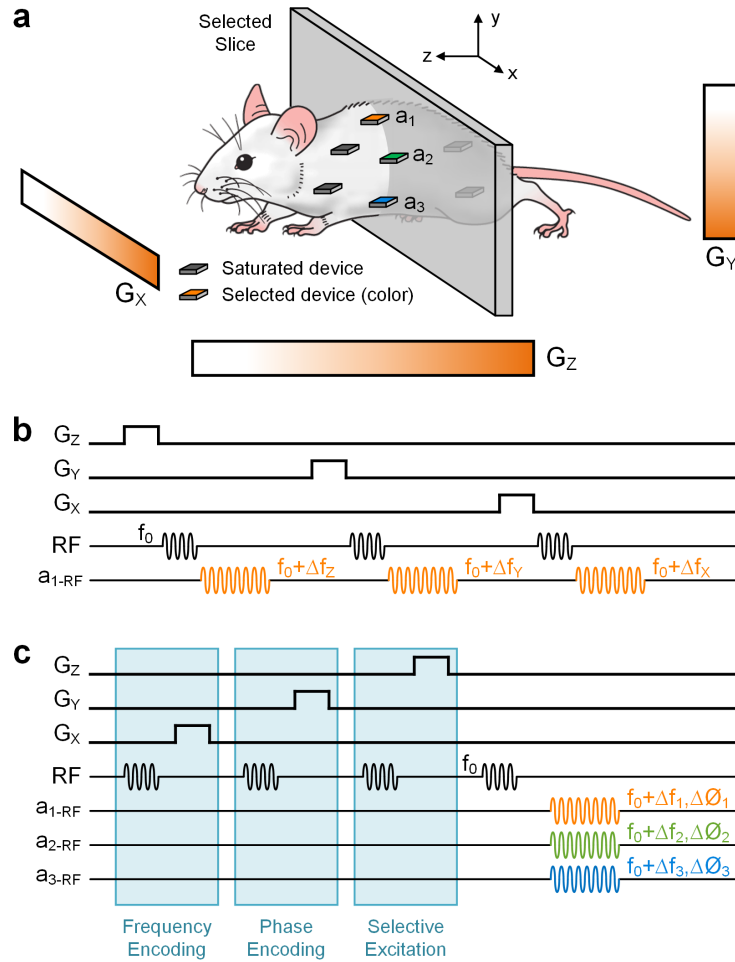
Supplementary Figure S2 – 3-D localization schemes. (**a**) Illustration for 3-D localization of ATOMS devices. G_X, G_Y and G_Z are the magnetic field gradients. (**b**) Pulse sequence for 3-D localization of a single device (a_1) using only frequency encoding. The frequency shifts after each RF excitation Δf_X, Δf_Y and Δf_Z are proportional to the local magnetic field generated by G_X, G_Y and G_Z, respectively. By mapping these frequency shifts back in space, the location of a_1 can be determined. (**c**) Pulse sequence for 3-D localization of multiple devices. ATOMS devices can be designed to expect four RF pulses before transmitting their responds. The first two pulses trigger the chips to sense the magnetic field generated by G_X and G_Y, and set Δf and $\Delta \phi$, respectively. The third pulse tells the devices to sense the field generated by G_Z and become silent during transmission if they experience a field magnitude above a certain threshold (outside the slice of interest). The final RF pulse is then used for frequency acquisition and synchronization, and to indicate devices not saturated by G_Z (selected devices a_1, a_2 and a_3) to start transmitting according to their frequency and phase shifts (Δf_1, Δf_2, Δf_3, and $\Delta \phi_1$, $\Delta \phi_2$, $\Delta \phi_3$, respectively). These frequency and phase shifts are then mapped back in space to estimate the location of selected devices.
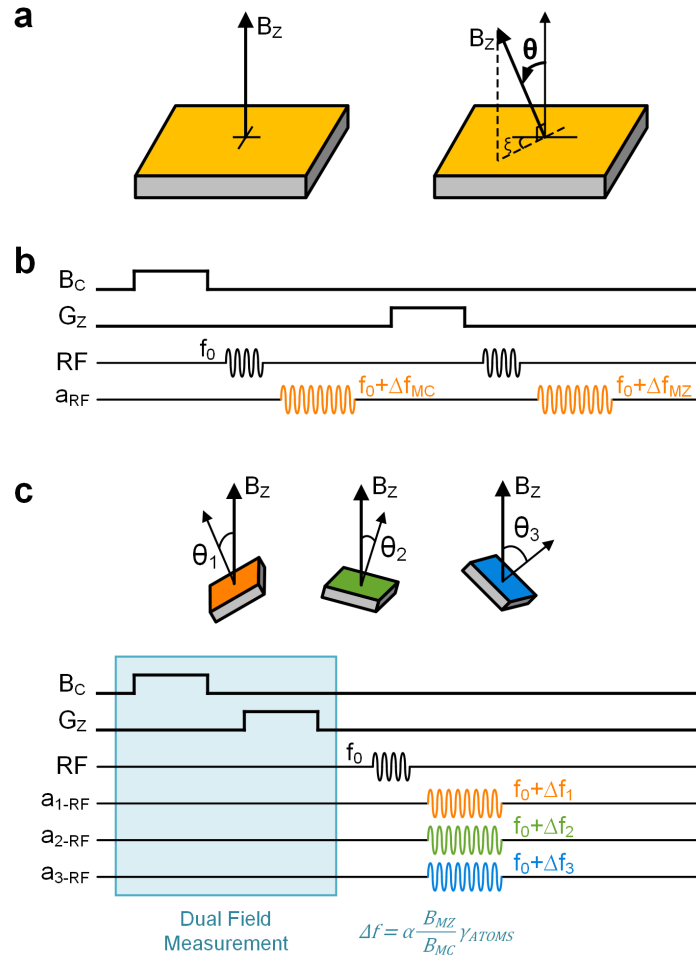
Supplementary Figure S3 – Compensation scheme for angular misalignment. (**a**) Illustration of angular misalignment, where θ is the azimuthal angle and ξ is the polar angle. In this case, the ATOMS device measures $B_Z \cos\theta$. (**b**) Pulse sequence for localization of a single device with angular misalignment. An extra step in the pulse sequence is added where a uniform magnetic field B_C is applied to measure a correction factor. This factor is used to estimate the local magnetic field generated by G_Z (B_{G_Z}) from measured frequency shifts Δf_{MC} and Δf_{MZ}, and the known field B_C. (c) Pulse sequence for localization of multiple arbitrarily aligned ATOMS devices. In this case, each device calculates the ratio of measured fields B_{MZ} and B_{MC}, and shifts its oscillation frequency in proportion to this ratio, γ_{ATOMS}, and the bandwidth utilization constant α.

References

1.   Herzel, F. An analytical model for the power spectral density of a voltage-controlled oscillator and its analogy to the laser linewidth theory. *IEEE Trans. Circuits Syst. I Fundam. Theory Appl.* **45,** 904–908 (1998).

2.   Navid, R., Lee, T. H. & Dutton, R. W. An analytical formulation of phase noise of signals with Gaussian-distributed jitter. *IEEE Trans. Circuits Syst. II Express Briefs* **52,** 149–153 (2005).

3.   Chorti, A. & Brookes, M. A spectral model for RF oscillators with power-law phase noise. *IEEE Trans. Circuits Syst. I Regul. Pap.* **53,** 1989–1999 (2006).